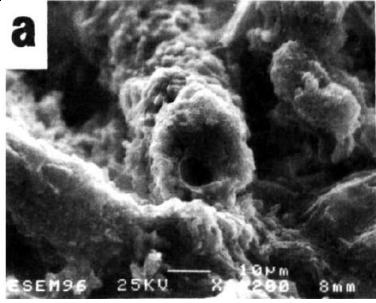
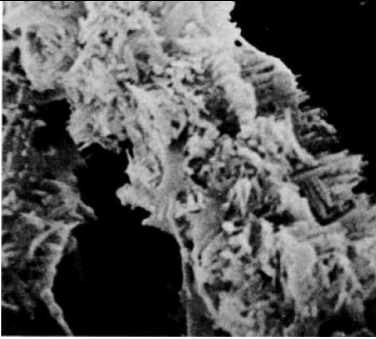
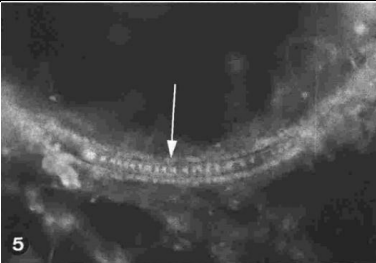
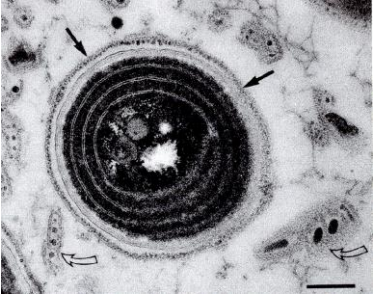
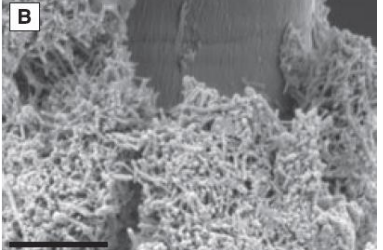
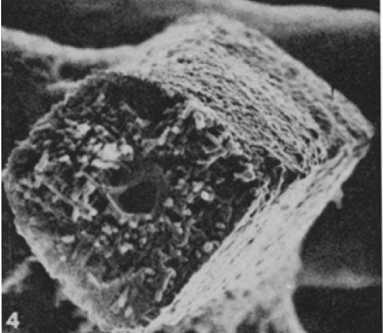
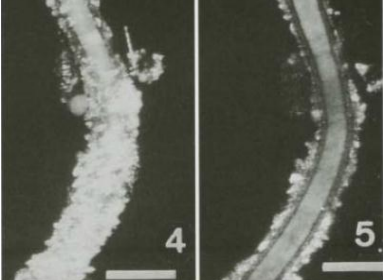
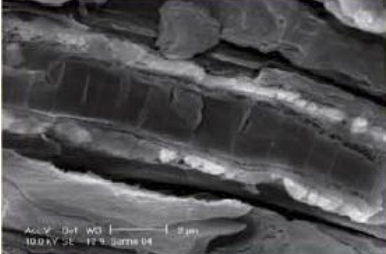
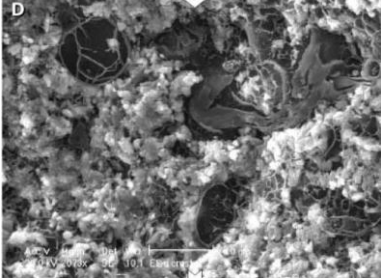
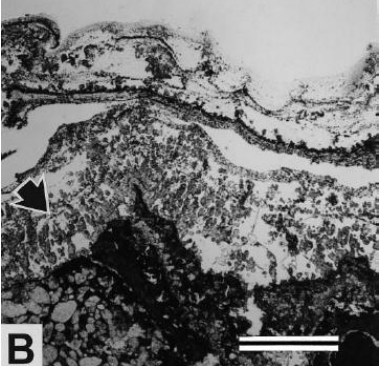
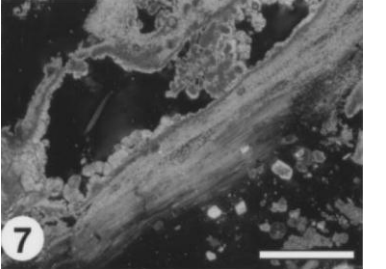
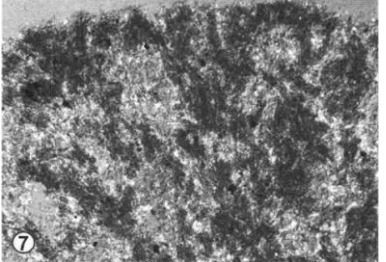
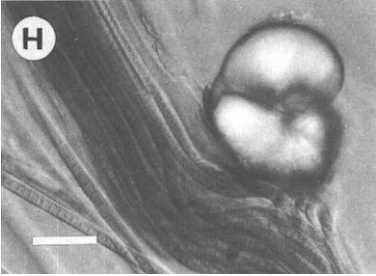
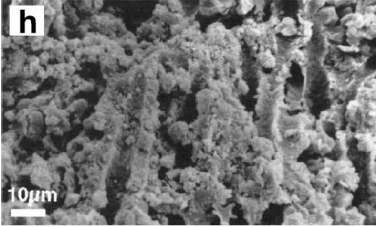
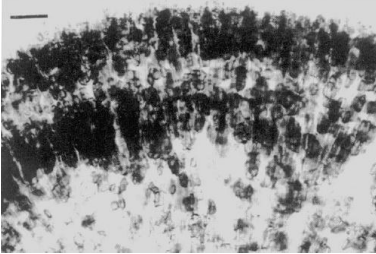
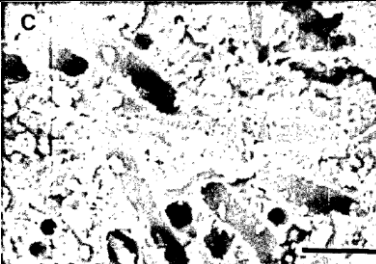
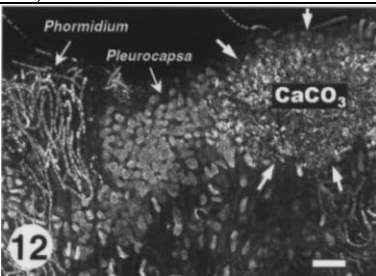


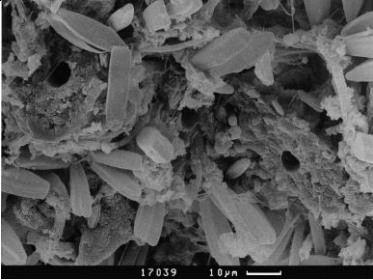
Table S1: Modern examples of cyanobacterial calcification from the literature. The calcification mechanism invoked is either direct calcification of cyanobacterial sheath (green), EPS replacement by carbonate (bleu) or undetermined (grey).

Location	Cyanobacteria	Mechanism	Mineral	Ref.	Picture
Rangiroa Atoll lacustrine stromatolite	<i>Scytonema mirabile</i>	Sheath calcification : metabolically mediated	Mg-calcite	(1)	 <p>SEM picture of calcified sheaths of filamentous cyanobacteria (from Defarge et al. 1994)</p>
Freshwater pool Aldabra, atoll Indian Ocean pH =7.5-8.6	<i>Plectonema gloeophilum</i>	Sheath calcification	calcium carbonate	(2)	 <p>SEM of calcified sheath of <i>Plectonema gloeophilum</i> Borzi from freshwater pool , west Island, Aldabra x5500 (from Riding 1977)</p>
Fresh water prairies in the Everglades, (Florida, USA)	<i>Scytonema</i> sp. And <i>Schizothrix</i> sp.	Sheath calcification (outer part of the sheath)	calcium carbonate	(3, 4)	 <p><i>Scytonema</i> sp. Epifluorescence micrograph Na<sub>2</sub>-Calcein stained mature filament. Arrow shows a dense cover of newly formed crystals with a blue/green fluorescence. Scale 5 μm. (From Thiel et al. 1997)</p>
Fayetteville Green Lake, New York. Investigating whittings events	<i>Synechococcus</i> strain GL24	Sheath calcification “The S-layer acts as a template for precipitation and, once it has become mineralized, is shed and replaced by a new S-layer”	calcite	(5)	 <p>Transmission electron micrograph of a stained, thin-sectioned <i>Synechococcus</i> cell strain GL24 showing the S-layer (solid arrows: bar scale = 100 nm). Note the S-layer material shed from the cell surface (open arrows) (from Thompson et al. 1997)</p>

<p><b>Bahamian stromatolite</b> (marine)</p>	<p><i>Dichothrix</i> sp.</p>	<p>Sheath calcification <i>"initial calcification occurs in living cyanobacteria and is photosynthetically induced"</i> (from Planavsky et al. 2009)</p>	<p>aragonite</p>	<p>(6)</p>	 <p>SEM of carbonate from calcified filaments.,scale bar 5µm (from Planavsky et al. 2009)</p>
<p><b>Caves , Vienne (France)</b> terrestrial, cave wall</p>	<p><i>Geitleria calcarea</i></p>	<p>Sheath calcification</p>	<p>calcium carbonate</p>	<p>(7)</p>	 <p>SEM picture of calcified filaments. Scale bar = 50µm (from Coute 1982)</p>
<p><b>Florida caverns</b> terrestrial (cave wall)</p>	<p><i>Geitleria floridana</i></p>	<p>Sheath calcification</p>	<p>unknown</p>	<p>(8)</p>	 <p>Calcified sheath of <i>Geitleria floridana</i>, SEM. Filament width 6µm. (From Imre Friedmann 1979)</p>
<p><b>Necropolis tomb of Carmone (Italy)</b> terrestrial (tomb wall)</p>	<p><i>Scytonema julianum</i> <i>Geitleria calcarea</i></p>	<p>Sheath calcification</p>	<p>calcite</p>	<p>(9)</p>	 <p>Confocal picture of a <i>Scytonema julianum</i> filament Scale bar : 25µm (from Arino et al. 1997)</p>
<p><b>Papoua New-Guinea aerophytic habitas</b> (tree trunks and limestone)</p>	<p><i>Scytonema</i></p>	<p>Sheath calcification</p>	<p>calcium carbonate (various morphology : acicular/tri radiate/dendritic)</p>	<p>(10)</p>	 <p>SEM of calcified <i>Scytonema</i> filament (Bar 5µm) (from Hoffman 1992)</p>

<p><b>Sarine river</b> (fresh running water)</p>	<p><i>Phormidium</i>, <i>Oscillatoria</i></p>	<p>Sheath calcification</p>	<p>calcium carbonate</p>	<p>(11)</p>	 <p>SEM picture of a calcified sheath of a filamentous cyanobacterium (scale bar = 2µm) (from Dupraz et al., 2009)</p>
<p><b>Hypersaline lake of Eulethera</b> (pH 9)</p>	<p>Cyanobacteria dominated biofilm (filamentous and coccoid)</p>	<p>EPS replacement by carbonate</p>	<p>high-Mg calcite</p>	<p>(11, 12)</p>	 <p>Photomicrographs showing microbial communities and microstructure of precipitates as seen with FEG-ESEM using cryofixation. (from Dupraz et al. 2004)</p>
<p><b>Pyramid Lake (USA)</b> alkaline (pH=9.3)</p>	<p><i>Phormidium</i> calcifying biofilm</p>	<p>EPS replacement by carbonate</p>	<p>calcium carbonate</p>	<p>(13, 14)</p>	 <p>EM micrograph of a Overview of a calcifying <i>Phormidium</i>-biofilm Scale bar = 10µm (from Arp et al. 1999b)</p>
<p><b>Lake Nuertu (China)</b> alkaline (pH=10)</p>	<p><i>Phormidium</i> calcifying biofilm</p>	<p>EPS replacement by carbonate</p>	<p>aragonite</p>	<p>(13)</p>	 <p>Microcrystalline laminae form at the border of shrinkage voids within the mucilaginous biofilm by spatial concentration and further growth of the initially precipitated aragonite crystals. Cross-polarized light. Scale bar represents 1 mm. (from Arp et al. 1999a)</p>
<p><b>Hard-Water Creek Deinschwanger Bach (Germany)</b> alkaline (pH 8.3)</p>	<p><i>Phormidium</i> <i>Pleurocapsa</i> biofilms</p>	<p>EPS replacement by carbonate</p> <p><i>“Though the initial process of external nucleation on cyanobacterial sheaths in the however creek section might be promoted of by a photosynthetically induced microscale pH gradient, the effect is not strong enough to cause a CaCO<sub>3</sub></i></p>	<p>calcium carbonate</p>	<p>(15)</p>	

		impregnation of the sheaths." (from Arp et al. 2001)			Surface part of a tufa biofilm crust sampled View showing dark, micritic encrustations of the bush-like filament arrays of <i>Phormidium incurvatum</i> . Nomarski optics. (from Arp et al. 2001)
<b>Culture experiment (lab)</b>	<i>Microcoleus</i> sp.	EPS replacement by carbonate <i>Spherulite nucleation and growth in the cell vicinity</i>	low-Mg calcite	(16)	 <p>Binocular microscope view of an in vitro spherulite associated with <i>Microcoleus</i> sp. Trichomes Scale bar : 40µm (from Verrechia et al. 1995)</p>
<b>Tufa-depositing stream in SW Japan (Shirokawa)</b>  alkaline	<i>Lyngbya</i> , <i>Phormidium</i>  <i>Symploca</i>	"We infer that the increased precipitation rate (summer-autumn) stimulated thick calcite encrustation on cyanobacterial filaments" (from Kano et al. 2003)	calcite	(17)	 <p>SEM image of a dense lamina with traces of filaments thickly calcified by microcrystalline calcite (from Kano et al. 2003)</p>
<b>Streams North Yorkshire</b>  (shallow calcareous water derived from the Carboniferous Limestone formation)	<i>Rivularia haematites</i>	"Thus, two different processes of calcification may be operating: (i-80%), caused by the reduction in trichome growth and gel production allowing development of a surface precipitate; (ii-20%), calcification promoted by photosynthesis" (from Pentecost 1987)	calcite	(18)	 <p>Structure of <i>Rivularia</i> colonies from Mastiles West stream. Hand section from a colony grown on the cut block. Note prominent bands of calcification. (bar 100 µm.) (from Pentecost 1987)</p>
<b>Travertine from cascades in the Fleinsbrunn enbach (Germany)</b>	<i>Lyngbya</i> ( <i>Phormidium</i> ) <i>incurvatum</i>	"Microniches more favorable to photocalcification consist of groups of three or more trichomes lying side by side, enclosing narrow tubes of interstitial water." (From Pentecost 1995)	Calcium carbonate	(19)	 <p>Scanning electron micrograph of a sagittal section of travertine from the Fleinsbrunn enbach at ~2 mm depth, showing impressions of <i>Lyngbya</i> trichomes in the travertine matrix (Bar 10µm) (From Pentecost 1995)</p>
<b>Lake Satonda</b>  alkaline (pH =8.3)	<i>Phormidium</i> <i>Calothrix</i> <i>Pleurocapsa</i> biofilm	<b>"Discussed</b> <i>Biofilm calcification : replacement of EPS by carbonate</i> (Arp et al.) Or <i>"Periodic in vivo calcification of surfaces of subglobular cyanobacterial aggregates by Mg</i>	calcium carbonate	(13, 20–23)	 <p>Microcrystalline carbonate aggregate at the top of a <i>Phormidium</i> + <i>Calothrix</i> + <i>Pleurocapsa</i> biofilm. Note that living cyanobacteria (<i>Phormidium</i>, <i>Pleurocapsa</i>)</p>

		<i>calcite</i> " (Kazmierczak et al.)		remain free of precipitates, whereas the carbonate (area marked by arrows) nucleates within the EPS in no particular relationship to them. Overlay of an epifluorescence and crossed nicols. Scale bar represents 25 µm (from Arp et al. 1999a)
<b>Calcareous freshwater streams Bad Urach (Germany)</b>  pH=8, tufa formation	<i>Phormidium (Lyngbya) incrustatum</i>	"Calcium carbonate impregnation of cyanobacterial sheaths has not been observed" (from Merz-Preiss et Riding 1999)	calcium carbonate (24)	
	<i>Phormidium (Lyngbya) sp.</i>			
	<i>Aphanocapsa endolithica</i>			
	<i>Hyella fontana</i>			Broken tubiform crusts around two cyanobacterial filaments in tufa. These crusts are external encrustations around the outer surfaces of the sheaths. Specimen critical-point dried. (from Merz-Preiss et Riding 1999)

## References

- Defarge C, Trichet J, Coute A (1994) On the appearance of cyanobacterial calcification in modern stromatolites. *Sedimentary geology* 94:11–19.
- Riding R (1977) Calcified plectonema (Blue-green algae), a recent example of Girvanella from Aldabra atoll. *Palaeontology* 20:33–46.
- Thiel V, Merz-preib M, Reitnet J, Michaelis W (1997) Biomarker Studies on Microbial Carbonates : Extractable Lipids of a Calcifying Cyanobacterial Mat ( Everglades , USA ). *Facies* 36:163–172.
- Merz MUE (1992) The Biology of Carbonate Precipitation by Cyanobacteria. *Facies* 26:81–101.
- Thompson JB, Schultze-Lam S, Beveridge TJ, Des Marais DJ (1997) Whiting events: biogenic origin due to the photosynthetic activity of cyanobacterial picoplankton. *Limnology and oceanography* 42:133–41.
- Planavsky N, Ginsburg RN (2009) Taphonomy of Modern Marine Bahamian Microbialites. *Palaos* 24:5–17.
- Couté A (1982) Ultrastructure d'une cyanophycée aérienne calcifiée cavernicole: *Geitleria calcarea* Friedmann. *Hydrobiologia* 97:255–274.
- Imre Friedmann E (1979) The genus *Geitleria* (Cyanophyceae or Cyanobacteria) : Distribution of *G. calcarea* and *G. floridana* n. sp. *Pl Syst Evol* 131:169–178.
- Arino X, Hernandez-Marine M, Saiz-Jimenez C (1997) Colonization of Roman tombs by calcifying cyanobacteria. *Phycologia* 36:366–373.
- Hoffmann L (1992) Variability in the crystal morphology of calcified terrestrial scytonema populations ( Cyanobacteria , cyanophyceae ). *Geomicrobiology journal* 10:59–64.
- Dupraz C et al. (2009) Processes of carbonate precipitation in modern microbial mats. *Earth-Science Reviews* 96:141–162.
- Dupraz C, Visscher PT, Baumgartner LK, Reid RP (2004) Microbe-mineral interactions: early carbonate precipitation in a hypersaline lake (Eleuthera Island, Bahamas). *Sedimentology* 51:745–765.
- Arp G, Reimer A, Reitner J (1999) Calcification in cyanobacterial biofilms of alkaline salt lakes. *European Journal of Phycology* 34:393–403.
- Arp G, Thiel V, Reimer A, Michaelis W, Reitner J (1999) Biofilm exopolymers control microbialite formation at thermal springs discharging into the alkaline Pyramid Lake, Nevada, USA. *Sedimentary Geology* 126:159–176.
- Arp G, Wedemeyer N, Reitner J (2001) Fluvial Tufa Formation in a Hard-Water Creek (Deinschwanger Bach, Franconian Alb, Germany). *Facies* 44:1–22.
- Verrecchia EP, Freytag P, Verrecchia KE, Dumont J-L (1995) Spherulites in calcrete Laminar Crusts : biogenic CaCO<sub>3</sub> precipitation as a major contribution to crust formation. *Journal of sedimentary research* A65:690–700.
- Kano A, Matsuoka J, Kojo T, Fujii H (2003) Origin of annual laminations in tufa deposits, southwest Japan. *Palaeogeography, Palaeoclimatology, Palaeoecology* 191:243–262.
- Pentecost A (1987) Growth and Calcification of the Freshwater Cyanobacterium *Rivularia haematites*. *Proceedings of the Royal Society of London Series B Biological Sciences* 232:125–136.
- Pentecost A (1995) Significance of the biomineralizing microniche in a lyngbya ( cyanobacterium ) travertine. *Geomicrobiology journal*:213–222.
- Kazmierczak J (1992) Recent Counterparts of Cyanobacterial Related Wetheredella and Paleozoic Problematic Fossils. *Palaos* 7:294–304.
- Arp G, Reimer A, Reitner J (2003) Microbialite formation in seawater of increased alkalinity, Satonda crater lake, Indonesia. *Journal of Sedimentary Research* 73:105–127.
- Arp G, Reimer A, Reitner J (2004) Microbialite formation in seawater of increased alkalinity, Satonda crater lake, Indonesia — REPLY. *Journal of sedimentary research* 74:318–325.
- Kazmierczak J, Kempe S (2004) Microbialite formation in seawater of increased alkalinity, Satonda Crater Lake, Indonesia - Discussion. *Journal of Sedimentary Research* 74:314–317.
- Merz-Preiss M, Riding R, Merz-Preiß M (1999) Cyanobacterial tufa calcification in two freshwater streams: ambient environment, chemical thresholds and biological processes. *Sedimentary Geology* 126:103–124.

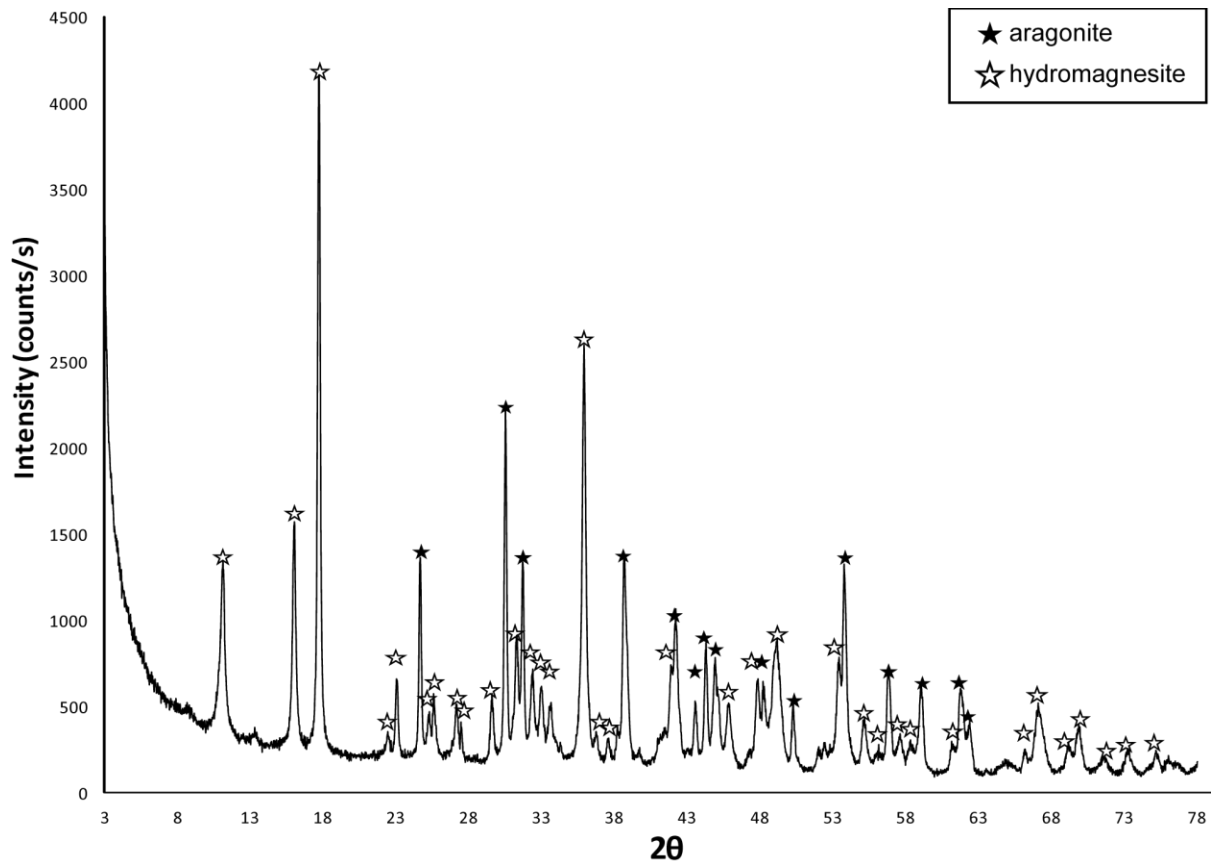


Figure S1: X-ray diffractogram of the 4 m-deep microbialite sample. Peaks assigned to hydromagnesite are marked with a black star; peaks assigned to aragonite are marked with a white star

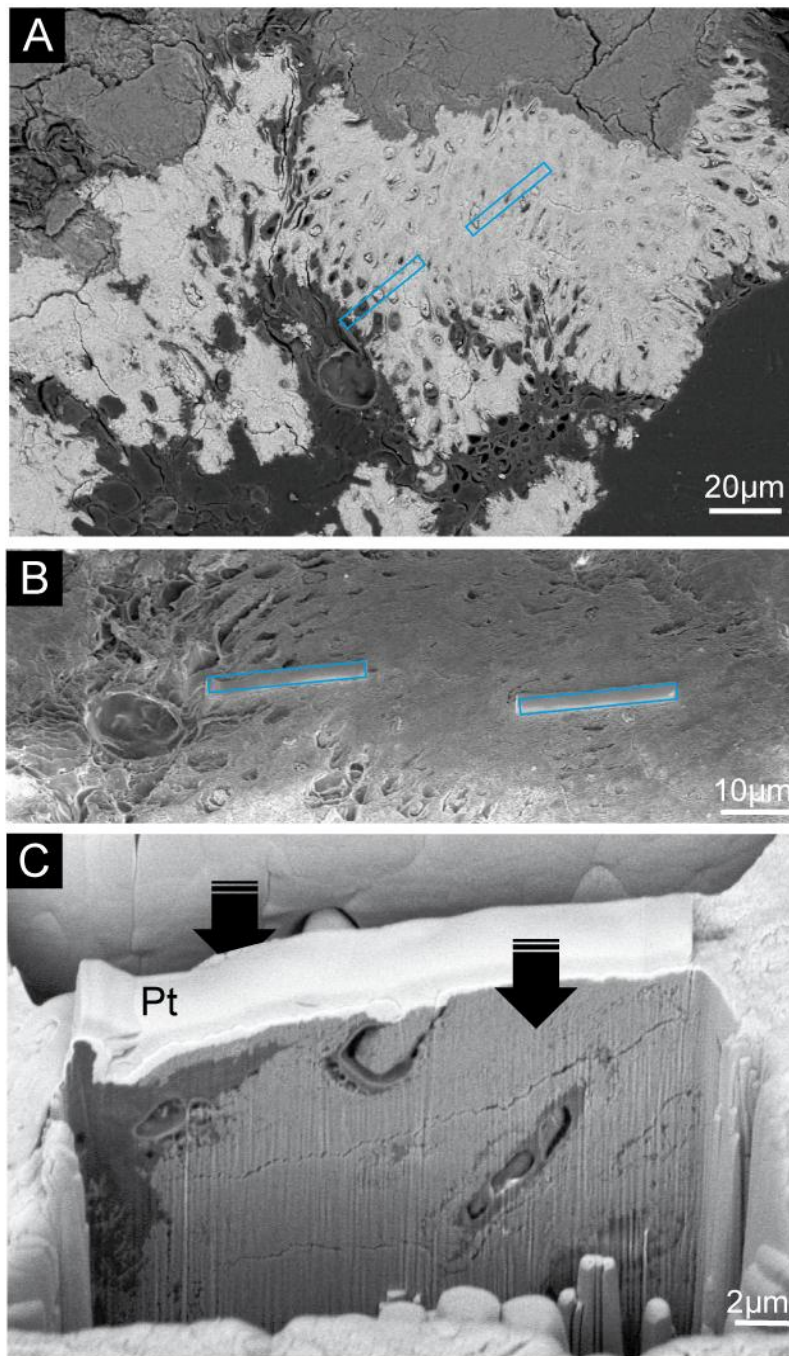


Figure S2: Milling of FIB foils. (A) SEM picture (backscattered electron mode) showing the location of FIB foils A and B. (B) SEM picture (In lens mode) showing where platinum straps were deposited. (C) SEM picture (secondary electron mode) of FIB foil A during the milling process. The ion beam removes matter from both sides of the foil (black arrows) which is protected by the platinum layer (Pt). Sections of Pleurocapsales cells are visible on the foil.

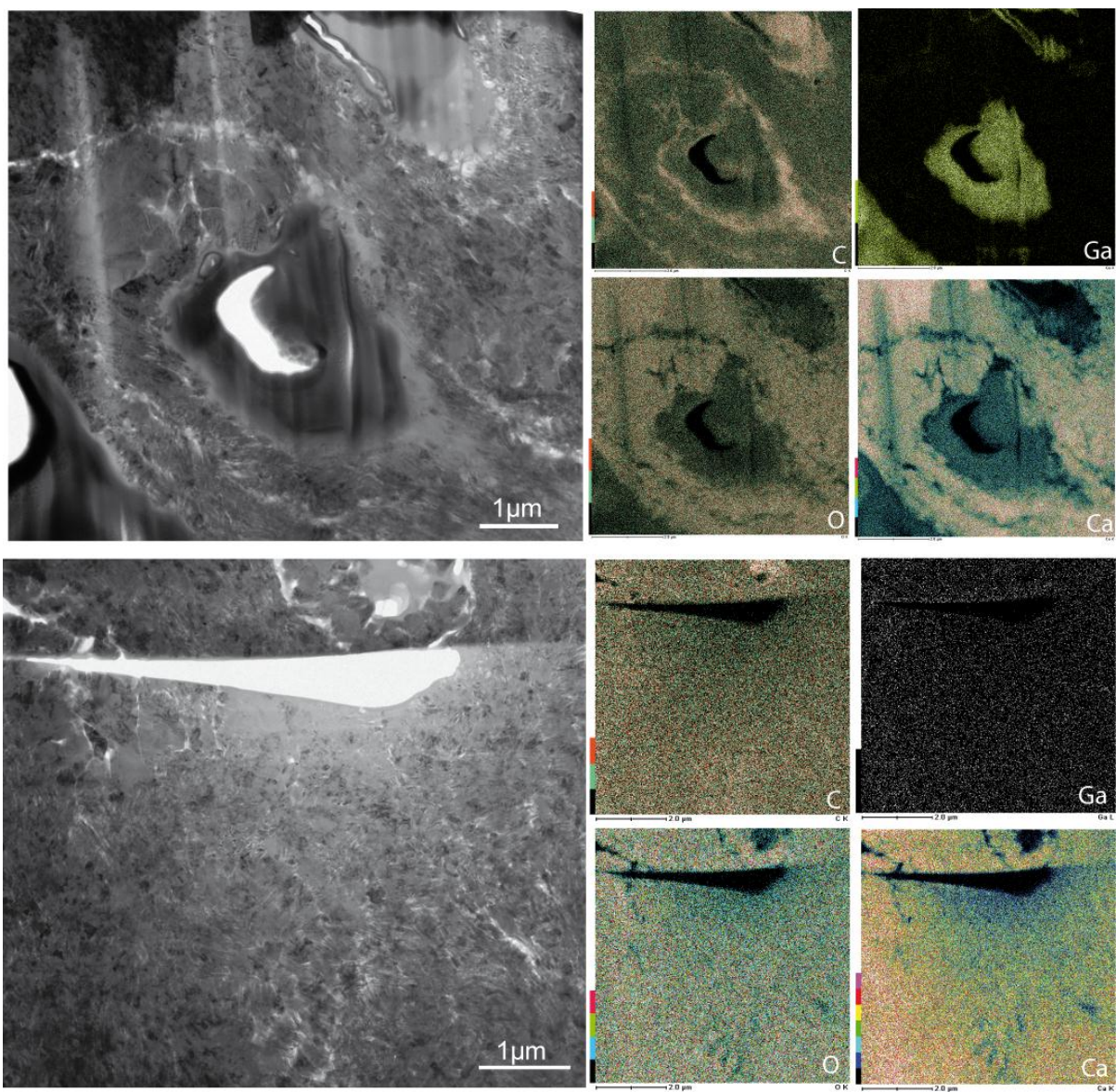


Figure S3: EDX analyses of FIB foils A and B. TEM pictures of FIB foils A and B, and corresponding EDX maps of carbon, gallium, oxygen and calcium.

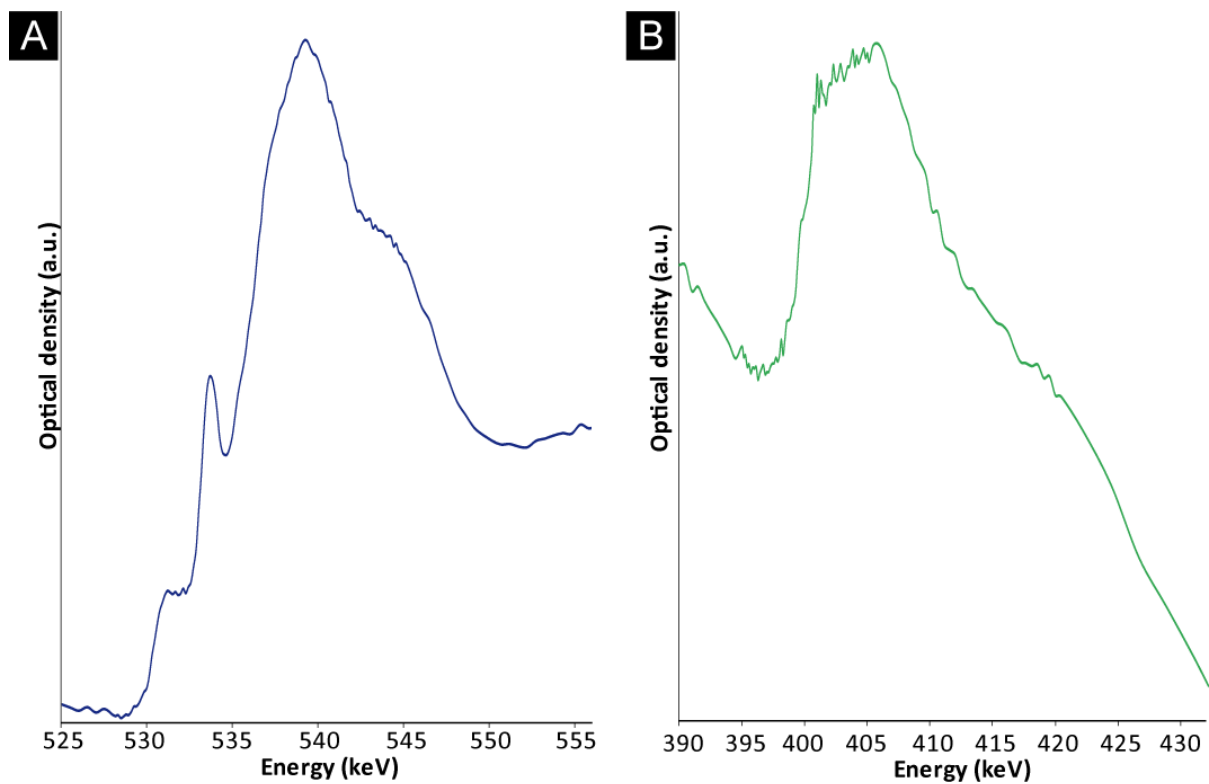


Figure S4: NEXAFS spectra at the O K-edge (A) and N K-edge (B) on organic matter composing the cells. Spectra extracted from FIB foil A analysis, spectroscopic signature of organic matter in the FIB foil B was identical.

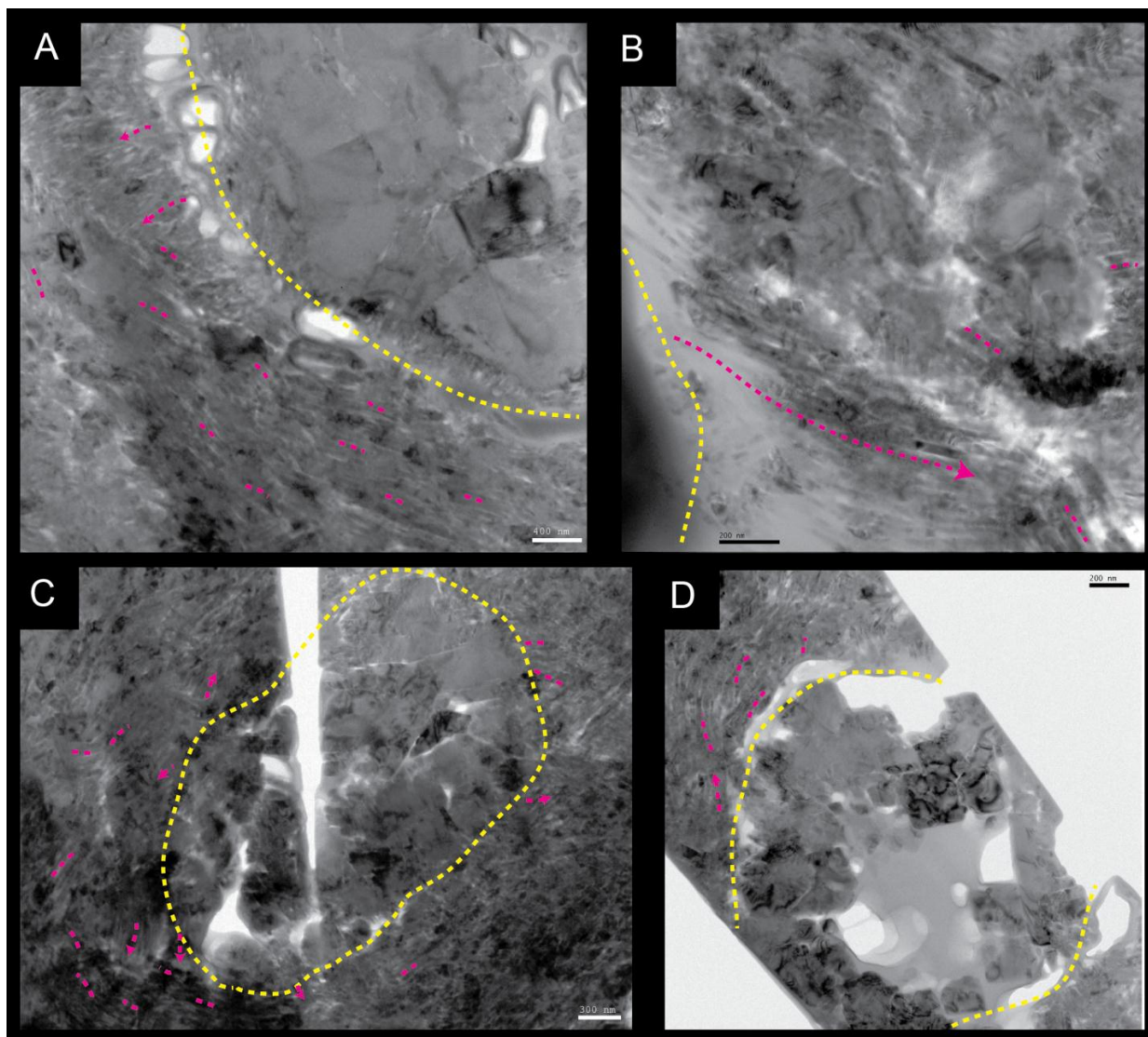


Figure S5: Bright field TEM pictures of FIB slice A (panels A and B) and B (panels C and D). The yellow dotted lines underline the putative limit of microfossil based on textural transition from type 1 aragonite to type 2 aragonite. The main crystallographic directions of aragonite type 1 clusters are underlined by pink dotted lines.

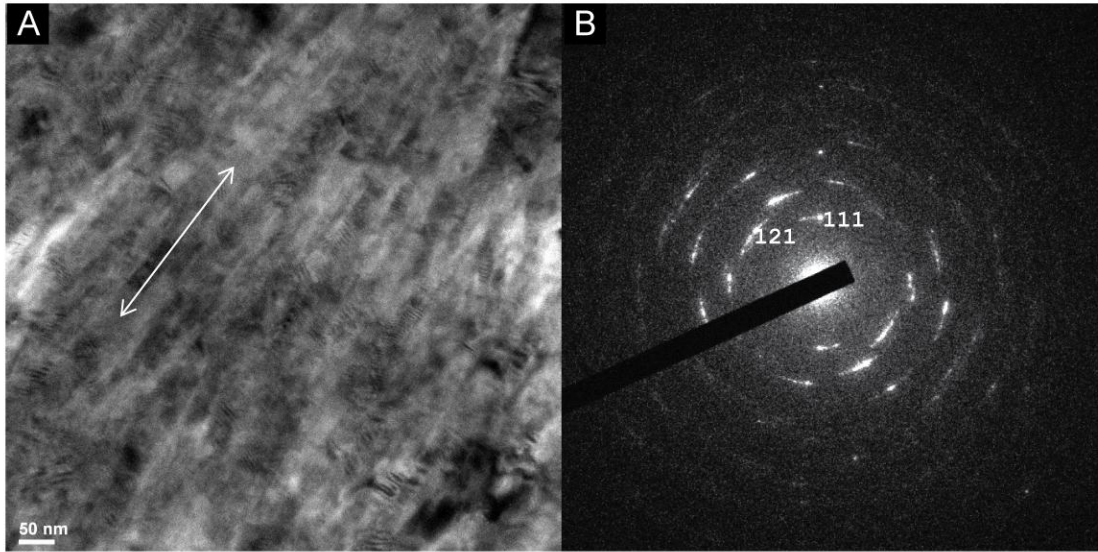


Figure S6: Electron diffraction pattern of Type 1 aragonite. (A) TEM picture of the area where the diffraction pattern was measured. A preferential orientation of aragonite needles (white arrow) is visible. (B) Diffraction pattern showing arcs of restricted angular stretch suggesting the presence of well crystallized aragonite nanocrystals with a preferential crystallographic orientation.

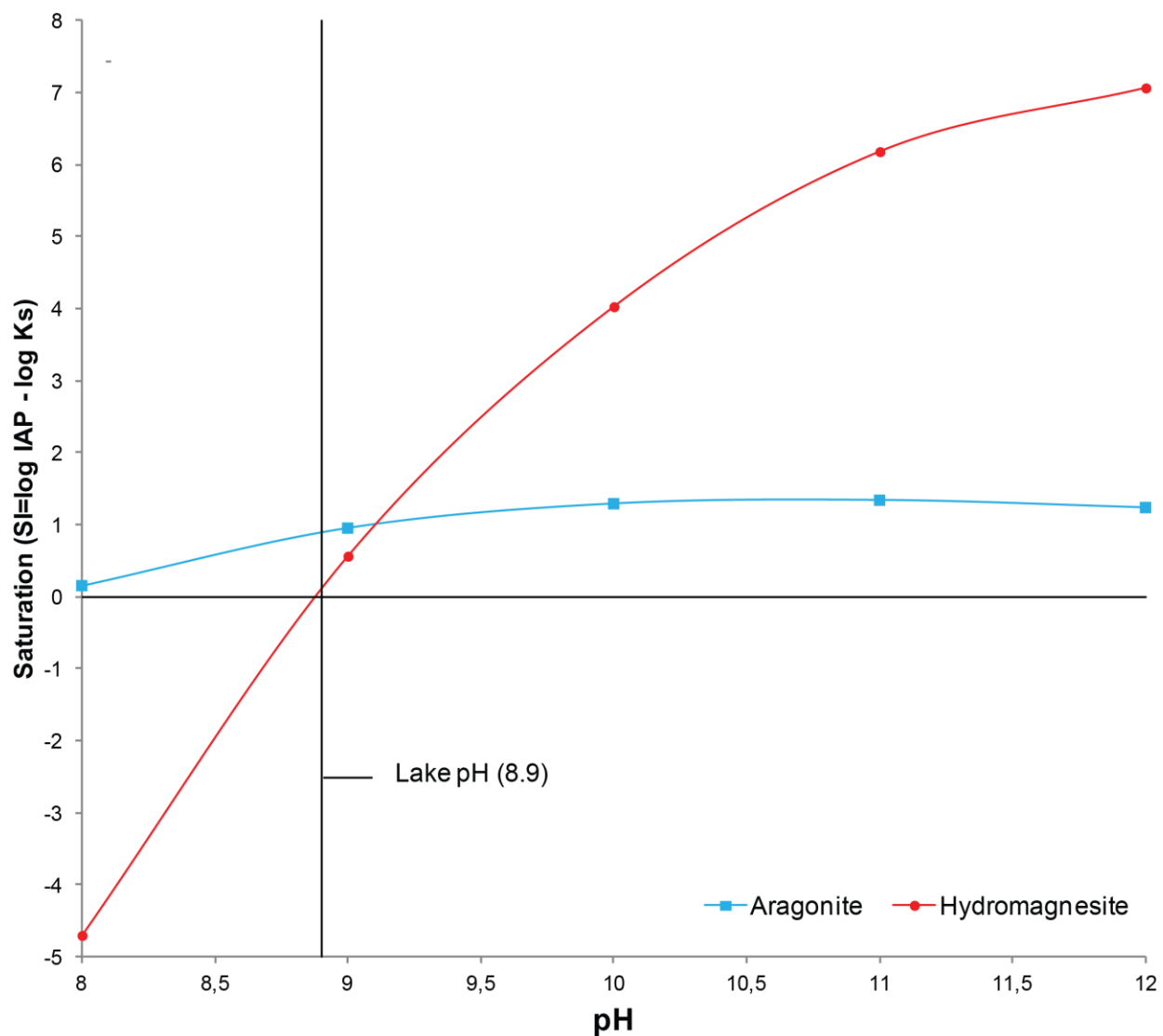


Figure S7: Evolution of saturation index of aragonite and hydromagnesite with pH. Calculations were performed based on the water lake chemistry published in (Kaźmierczak J et al. (2011) *Hydrochemistry and microbialites of the alkaline crater lake Alchichica, Mexico. Facies*)